Asian Journal of Chemistry; Vol. 32, No. 11 (2020), 2855-2859

ASIAN JOURNAL OF CHEMISTRY

https://doi.org/10.14233/ajchem.2020.22859

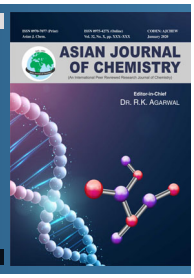

Synthesis and Catalytic Properties of Ruthenium and Iron Nanoparticles/Mesoporous Carbon Composites

YANMIN HOU*, XIAOJUN ZHAO and HAO LI

School of Chemistry and Chemical Engineering, Pingdingshan University, 467000 Henan, P.R. China

*Corresponding author: Fax: +86 375 2657600; Tel: +86 375 2657620; E-mail: hympdsu@163.com

Received: 16 June 2020; *Accepted*: 13 August 2020; *Published online*: 28 October 2020; AJC-20108

The mesoporous carbon material of Fe-MC loaded iron nanoparticles was obtained by pyrolysis of Fe-MIL-88A under nitrogen and reducing gas atmosphere. Addition of Ru(III) in the liquid phase, Ru(III) was reduced to ruthenium nanoparticles (RuNPs) by iron nanoparticles (FeNPs), led to the formation of mesoporous carbon composite of Ru@Fe-MC, where 0.77 wt% of Ru was completely wrapped on the surface of iron nanoparticles. The hydrolysis performance of Ru@Fe-MC to aminoborane was studied and the results showed a good catalytic performance, where the conversion frequency (TOF) was found to be 234.3 mol H_2 min^{-1} (mol Ru)$^{-1}$, and the activation energy was 33.6 kJ / mol. The reusbility catalyst performance of Ru@Fe-MC remained highly active after ten experiments.

Keywords: Ruthenium nanoparticles, Iron nanoparticles, Mesoporous carbon composites, Aminoborane, Catalytic properties.

INTRODUCTION

Ruthenium nanoparticles are widely concerned because of their outstanding catalytic performance in the process of aminoborane hydrolysis [1-4]. In order to solve the problem of ruthenium atom agglomeration on the catalyst support, enhance the catalytic activity and utilization efficiency, it is necessary to find a safe and effective support with low ruthenium nanoparticles loading, good dispersion and high catalytic activity. It has been found that there are several carriers which could help to disperse ruthenium nanoparticles, such as graphene [5], TiO_2 [6], MIL-53 (Cr, Al) [7], nickel nanoparticles [8], *etc*.

The metal organic framework compounds (MOFs) had the characteristics of high specific surface area and adjustable pore size [9-12], which could be transformed into mesoporous carbon materials and could be embed some transition metal nanoparticles evenly, such as nickel, aluminum, chromium, *etc*. These transition metal nanoparticles could selectively reduce precious metals under specific thermal cracking conditions [13]. Iron nanoparticles is a kind of highly magnetic metallic material. The introduction of catalyst system could make the catalyst have magnetic properties, thus improving the chemical stability and recyclability of the catalyst. In present study, Ru(III) was reduced to ruthenium nanoparticles by magnetic iron nanoparticles and embedded into the structure of MOFs and ruthenium nanoparticles was wrapped on the surface of magnetic transition iron nanoparticles to obtain metal nanoparticles and mesoporous carbon composites of Ru@Fe-MC. The prepared Ru@Fe-MC showed good catalytic performance in the process of aminoborane hydrolysis. Therefore, it is necessary to develop a potential method to synthesized Ru metal catalyst by using magnetic mesoporous carbon material as the support, which could be applied to the production of hydrogen gas from aminoborane.

EXPERIMENTAL

Rotary evaporator (Gongyi Yuhua Instrument Co. Ltd.), tubular furnace (TE050 Aianm Technology Co. Ltd.), blast drying oven (DH-101 Tianjin Zhonghuan Experimental Electric Furnace Co. Ltd.), high speed centrifuge (LG-16w Beijing Jingli Centrifuge Co. Ltd.), ultrasonic cleaner (Gongyi Yuhua Instrument Co. Ltd.) and vacuum pump (Sencor Gongyi Yuhua Instrument Co., Ltd) were applied in this experimental work. The chemicals *viz*. aminoborane, *N*,*N*-dimethyl formamide, ruthenium chloride, fumaric acid and iron nitrate were procured from CP National Pharmaceutical Group Chemical Reagent Co. Ltd.).

Synthesis of Fe-MIL-88A: In a 500 mL round bottom flask, added 300 mL DMF in 6.4 g $Fe(NO_3)_3 \cdot 9H_2O$ and heated to 110 ºC in an oil bath and stirred continuously. After the complete dissolution of iron nitrate, 1.68 g of fumaric acid was slowly added and heated the solution at 110 ºC with continuous stirring for 1 h. The product was washed three times with ethanol and DMF solution respectively at the action of high-speed centrifuge, and then,dried in a vacuum drying oven at 45 ºC for 12 h. The dried Fe-MIL-88A was obtained by grinding in a mortar.

Synthesis of Fe-MC mesoporous carbon composite: Dried Fe-MIL-88A (2 g) was kept in the tubular furnace for thermal cracking. The setting conditions were optimized by introducing nitrogen gas. The heating rate was set as 5 º/min, and after heating to 700 ºC for 1 h, the temperature was allowed to decrease. Hydrogen (H_2/N_2 = 1:3, v/v) was introduced to the sample at 400 ºC for 2 h. In this process, iron ions were reduced to iron nanoparticles and Fe-MC was obtained at room temperature.

Synthesis of Ru@Fe-MC mesoporous carbon composite:. Dissolved 40 mL distilled water, 5 mL ethanol (added a small amount of ethanol to enhance the dispersion of Fe-MC in aqueous solution) and 500 mg Fe-MC in a 100 mL round bottom flask. Now, 12.5 mL of Ru(III) was added to the above mixture and vibrated for 30 min under the action of ultrasonic wave, and then stirred at room temperature under magnetic stirrer for 8 h. In this process, iron nanoparticles loaded on Fe-MC was used as the sole reductant to reduce Ru(III) to Ru, and Ru was wrapped on the surface of iron nanoparticles. Under the action of magnetic force, washed the catalyst with distilled water and ethanol for three times respectively, dried it in a vacuum drying oven at 45 ºC for 12 h and then grinded to get the dry catalyst Ru@Fe-MC.

Catalytic studies: Ru@Fe-MC (10 mg) was dispersed in 10 mL deionized water and transferred into a double necked round bottom flask, one neck was connected to the gas detection device and the other neck was introduced into the aqueous solution of aminoborane through a constant pressure funnel. When aminoborane solution in the constant pressure funnel was added to the double neck flask containing catalyst, the hydrolysis reaction occurred immediately and the volume of generated hydrogen was recorded at a specific time interval (30 s).

RESULTS AND DISCUSSION

P-XRD analysis: The synthesized Fe-MC and Ru@Fe-MC were characterized by powder X-ray diffraction. As shown in Fig. 1, the characteristic peaks at 44.7º and 65.0º of Fe-MC is observed. By comparing with JCPDS card No. 65-4899, it could be classified as the diffraction peaks of Fe (110) and Fe (200) crystal faces, respectively. Compared with the powder X-ray diffraction pattern of Fe-MC, there is an additional diffraction peak of elemental Ru (JCPDS no. 00-006-0663) at 2θ ~ 44º on Ru@Fe-MC, which indicated that the elemental Ru has been successfully grafted to the surface of iron nanoparticles and the characteristic peak of Ru was not obvious, which indicated that loaded ruthenium nanoparticles on Ru@Fe-MC is very small.

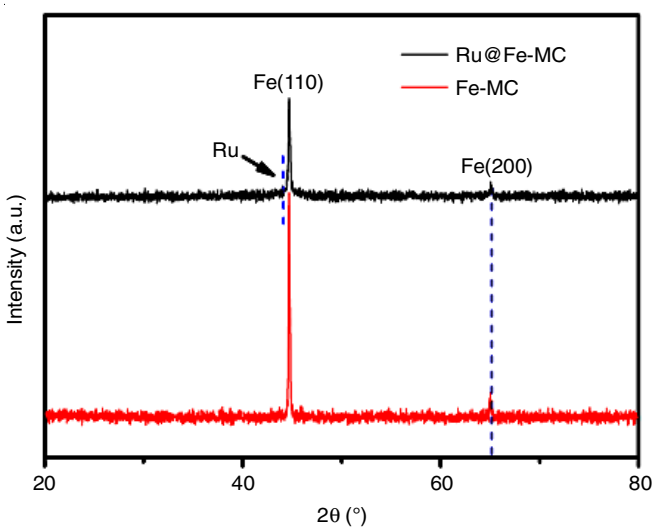

Fig. 1. XRD patterns of Ru@Fe-MC and Fe-MC nanocatalyst

SEM studies: The surface morphology of Fe-MIL-88A was studied by scanning electron microscope (SEM). As shown in Fig. 2a, the microstructure of Fe-MIL-88A indicated that it has the structure morphology of spindle, about 1.7 μm in length and about 1 μm in average width. Fig. 2b-c showed the Ru@Fe-MC before and after catalytic hydrogen production from aminoborane, respectively. After repeated use for 10 times, the morphology and structure of Ru@Fe-MC was almost unchanged.

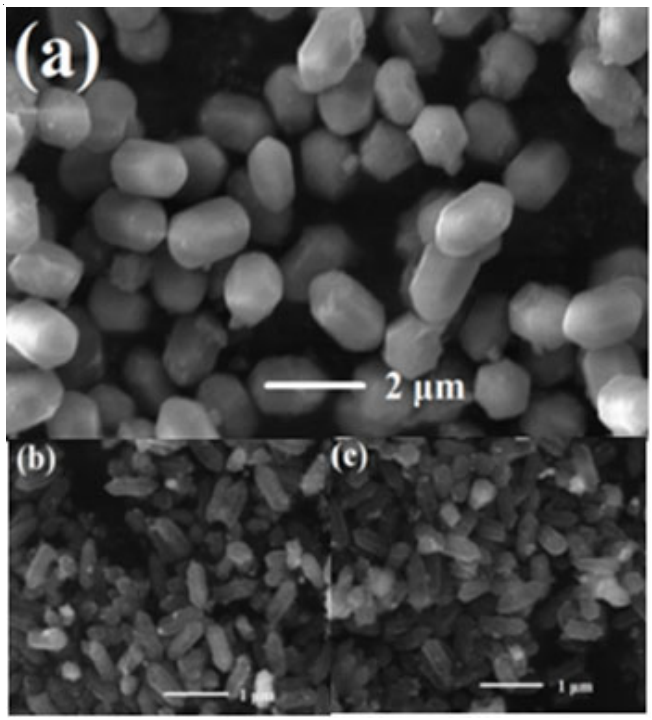

Fig. 2. (a) SEM images of Fe-MIL-88A, SEM images of Ru@Fe-MC (b) before catalytic reaction and (c) after the 10th cycle of reaction

TEM studies: Compared with the morphology and structure of Fe-MIL-88A, the spindle morphology of Fe-MC had almost no change after thermal cracking of Fe-MIL-88A, but

its length and width became about 1 μm and 330 nm (Fig. 3a-b). In addition, a uniform distribution of iron nanoparticles on mesoporous carbon materials was also observed. Fig. 3c indicated that Fe-MC was converted to Ru@Fe-MC by Ru grafting. In this process, the original morphology was still sustained. Fig. 3d showed the energy dispersive X-ray images of Ru@Fe-MC, where the characteristic peaks of C, Ru, Fe and Cu were clearly observed. This result showed that some iron nanoparticles and ruthenium has been embedded in the mesoporous carbon structure.

Magnetic characterization: The magnetism of Fe-MC and Ru@Fe-MC was measured by vibrating sample magnetometer. The saturation magnetization (Ms) was respectively 177 and 90 emu g^{-1} and coerceivity (HC) of the samples was 87 and 93 Oe, respectively. This indicated that Fe-MC and Ru@Fe-MC had strong magnetism.Therefore, the nanocatalyst of Ru@Fe-MC could be rapidly separated from the reaction mixture at the action of external magnetic force.

BET analysis: N_2 adsorption-desorption isotherms and pore size distribution of the Fe-MC and Ru@Fe-MC are shown in Fig. 4.The specific surface area of Fe-MC and Ru@Fe-MC was respectively 83.7 and 72.6 m^2 g^{-1}, which indicated that Fe-MC and Ru@Fe-MC contained a lot of pores. With Ru loading, the specific surface area of the sample decreased, which further showed that Ru has been loaded on the mesoporous material. The pore size of Fe-MC and Ru@Fe-MC was mainly concentrated at 8-48 nm and 8-42 nm, respectively (Fig. 4b). This may be because that the pore cavity of Fe-MC was embedded by ruthenium nanoparticles and some iron nanoparticles were wrapped by Ru atoms. The pore size of Ru@Fe-MC was slightly smaller than that of Fe-MC.

Catalytic hydrolysis of aminoborane: According to the test method, under the same conditions, the catalytic activity of Ru@Fe-MC and Fe-MC was studied. The performance curve of hydrogen production by hydrolysis of aminoborane is shown in Fig. 5, this experiment was performed at the atmospheric pressure and temperature of 25 ± 0.2 ºC, aminoborane concentration was 58.90 mmol and the dosage of Ru@Fe-MC and Fe-MC was 6 mg. The results showed that hydrogen gas was released immediately by Ru@Fe-MC, while no hydrogen was evolved within 11 min when Fe-MC as catalyst. It could be seen that ruthenium was the only active factor to catalyze the hydrolysis of aminoborane to produce hydrogen gas.

Effect of catalyst dosage: Under the optimized conditions, different dosage of Ru@Fe-MC *viz*. 4 mg, 6 mg and 8 mg at 25 ± 0.2 ºC and normal pressure, the catalyst was dispersed

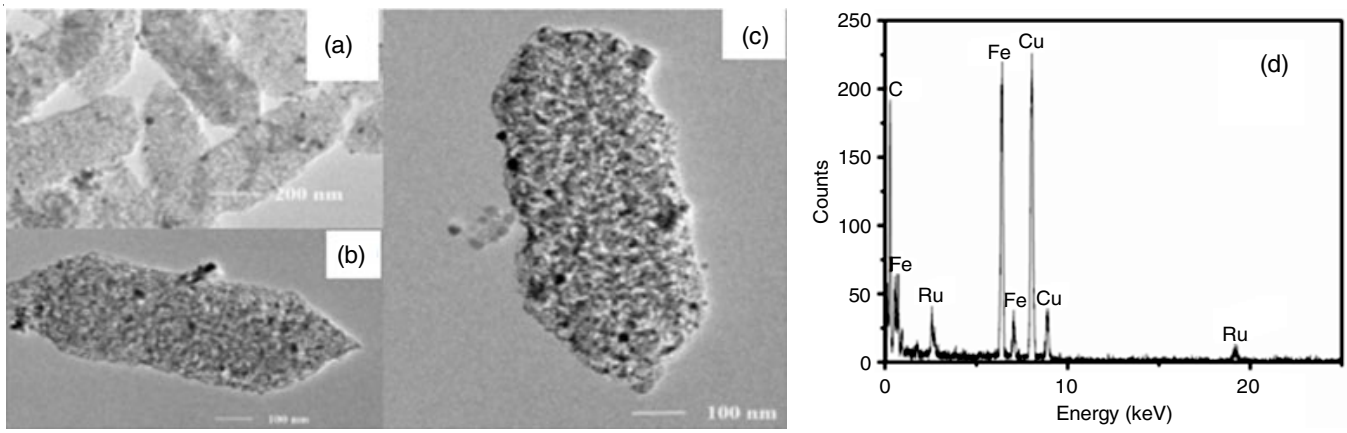

Fig. 3. (a and b) TEM images of Fe-MC, (c) TEM images of Ru@Fe-MC, (d) EDS spectra of Ru@Fe-MC

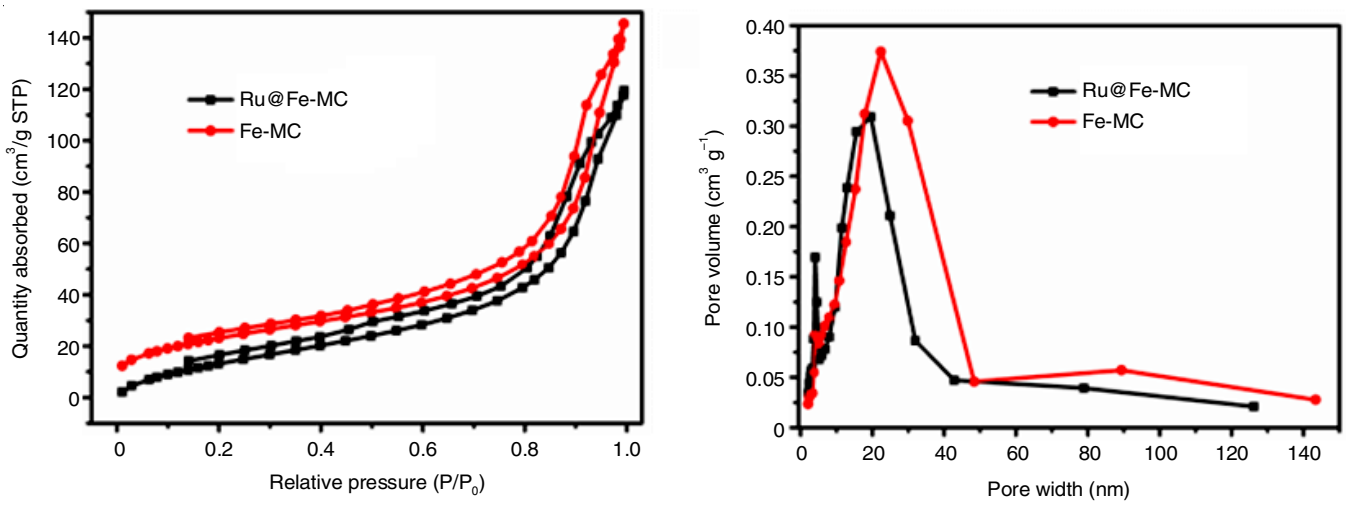

Fig. 4. (a) N_2 sorption isotherms of Fe–MC and Ru@Fe–MC;(b) pore size distribution of Fe–MC and Ru@Fe–MC

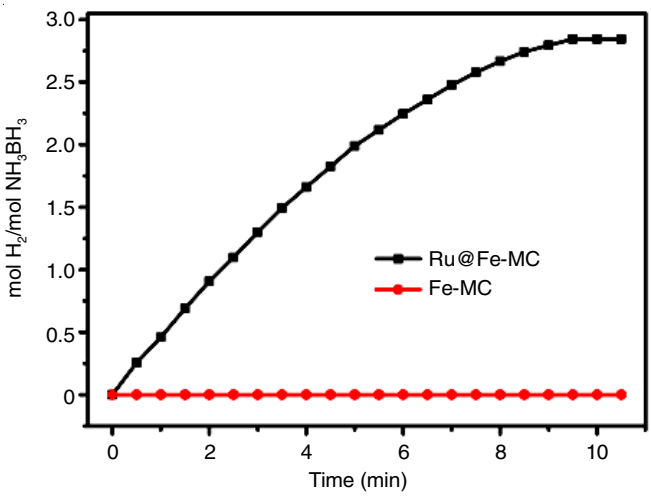

Fig. 5. Hydrogen generation from the hydrolysis of aminoborane catalyzed by Ru@Fe-MC and Fe-MC catalyst at 25 ± 0.2 °C, [aminoborane] = 58.90 mM

into 5 mL of distilled water, ultrasonated for 5 min, followed by the addition of 10 mg of aminoborane. The scale of burette was recorded when the first bubble came out, noted after every 30 s until the reaction stops. It can be seen from Fig. 6 that the mole ratio of aminoborane to hydrogen released increases with the change of time and the larger was close to 3. The results showed that the hydrolysis rate of aminoborane increased with the increase of the amount of catalyst.

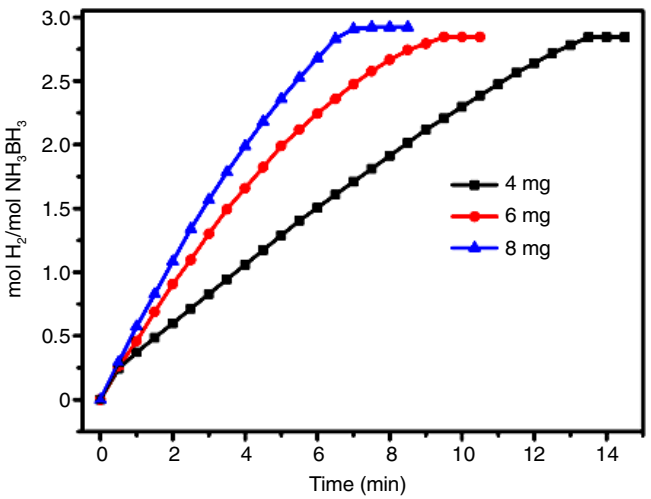

Fig. 6. Time courses for hydrogen production from hydrolysis of aminoborane using different catalyst dosage at 25 ± 0.2 ºC, [aminoborane] = 58.90 mM

Effect of different concentration of aminoborane: Under optimzed conditions, different volume of aqueous solution of aminoborane (0.2, 0.3, 0.4 and 0.5 mL) was added separately. The gas volume was recorded when the first bubble of hydrogen was released from the solution. From Fig. 7, it is found that the final volume of hydrogen released from aminoborane also increased with the increase of the concentration of aminoborane, but the slope of time and volume of hydrogen remained almost the same.This indicated that the hydrolysis of aminoborane is a quasi-zero order reaction.

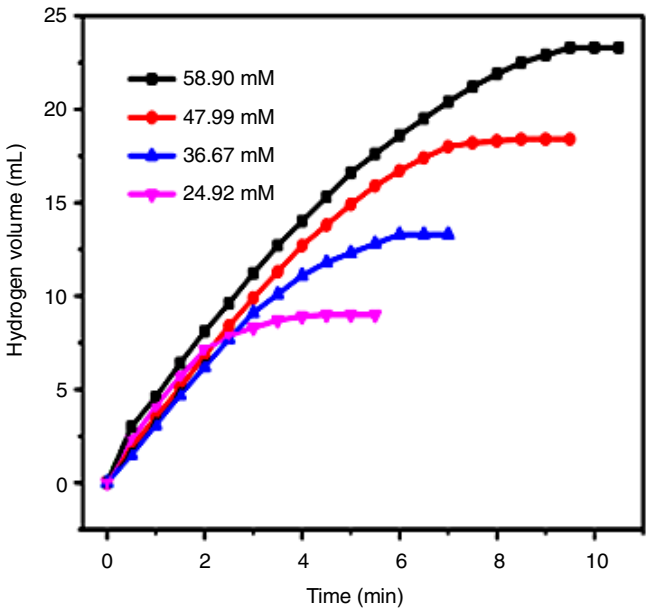

Fig. 7. Time courses for hydrogen production from hydrolysis of aminoborane using different aminoborane concentrations at 25 ± 0.2 °C

Effect of temperature: Under the optimized experimental conditions, the effect of different temperatures on the hydrolysis of aminoborane is also investigated. The results showed that the dehydrogenation rate of aminoborane was different at different temperatures. With the increase of temperature, the dehydrogenation rate increased rapidly. According to the dehydrogenation curve, the constant k of dehydrogenation rate at different temperatures could be obtained. Fitting ln K and ln (T/1), the activation energy was 33.6 kJ mol^{-1}, which was lower than the activation energy of other catalysts reported in the literature.

Reusability of catalyst: Under the optimized conditions, the device remained unchanged, the catalyst was not separated, and repeated the circulation for 10 times. The results showed that the hydrolysis rate of aminoborane decreases slowly with the increase of circulation times and the catalytic activity of Ru@Fe-MC decreased slightly. One of the reasons may be attributed that a small amount of catalyst sticks to the wall of the round bottom flask and did not dispersed in the solution when the magnon was stirred, which was confirmd with the ICP-AES data after the reaction, the content of ruthenium was found to be 0.63 wt% of Ru@Fe-MC. During the reaction, the active factor of ruthenium may be partially oxidized or lost, however, before and after the reaction, the morphology and structure of Ru@Fe-MC were almost unchanged, and the dispersion of metal nanoparticles was still very good.

Conclusion

The mesoporous carbon materials had the advantages of large specific surface area, large number of pore size, simple synthesis and so on, which was conducive to the dispersion of nanoparticles and the infiltration of aminoborane solution, and was a relatively promising carrier. The hydrolysis performance of Ru@Fe-MC to aminoborane showed good catalytic performance, the conversion frequency (TOF) was 234.3 mol H_2

min^{-1} $(mol\ Ru)^{-1}$ and the activation energy was 33.6 kJ / mol. The catalyst remains highly active after ten experiments. Since, Ru@Fe-MC has strong magnetism and low activation energy, so it may have certain potentialability as alloy catalyst.

CONFLICT OF INTEREST

The authors declare that there is no conflict of interests regarding the publication of this article.

REFERENCES

1. S. Akbayrak, Y. Tonbul and S. Ozkar, *Dalton Trans.*, **45**, 10969 (2016); https://doi.org/10.1039/C6DT01117A
2. Z. Wu, Y. Duan, S. Ge, A.C.K. Yip, F. Yang, Y. Li and T. Dou, *Catal. Commun.*, **91**, 10 (2017); https://doi.org/10.1016/j.catcom.2016.12.007
3. M. Navlani-García, K. Mori, A. Nozaki, Y. Kuwahara and H. Yamashita, *Appl. Catal. A Gen.*, **527**, 45 (2016); https://doi.org/10.1016/j.apcata.2016.08.018
4. X. Xiong, L. Zhou, G. Yu, K. Yang, M. Ye and Q. Xia, *Int. J. Hydrogen Energy*, **40**, 15521 (2015); https://doi.org/10.1016/j.ijhydene.2015.09.095
5. Z. Novotny, F.P. Netzer and Z. Dohnálek, *Surf. Sci.*, **652**, 230 (2016); https://doi.org/10.1016/j.susc.2016.03.020
6. K. Mori, K. Miyawaki and H. Yamashita, *ACS Catal.*, **6**, 3128 (2016); https://doi.org/10.1021/acscatal.6b00715
7. K. Yang, L. Zhou, G. Yu, X. Xiong, M. Ye, Y. Li, D. Lu, Y. Pan, M. Chen, L. Zhang, D. Gao, Z. Wang, H. Liu and Q. Xia, *Int. J. Hydrogen Energy*, **41**, 6300 (2016); https://doi.org/10.1016/j.ijhydene.2016.02.104
8. H. Li, X. Li, Y. Hou and X. Zhao, *Asian J. Chem.*, **29**, 1447 (2017); https://doi.org/10.14233/ajchem.2017.20500
9. C. Du, J. Su, W. Luo and G. Cheng, *J. Mol. Catal. Chem.*, **383-384**, 38 (2014); https://doi.org/10.1016/j.molcata.2013.11.018
10. D. Lu, G. Yu, Y. Li, M. Chen, Y. Pan, L. Zhou, K. Yang, X. Xiong, P. Wu and Q. Xia, *J. Alloys Compd.*, **694**, 662 (2017); https://doi.org/10.1016/j.jallcom.2016.10.055
11. S. Roy, P. Pachfule and Q. Xu, *Eur. J. Inorg. Chem.*, 4353 (2016); https://doi.org/10.1002/ejic.201600180
12. J. Chen, G. Xia, P. Jiang, Y. Yang, R. Li, R. Shi, J. Su and Q. Chen, *ACS Appl. Mater. Interfaces*, **8**, 13378 (2016); https://doi.org/10.1021/acsami.6b01266
13. W. Xia, C. Qu, Z. Liang, B. Zhao, S. Dai, B. Qiu, Y. Jiao, Q. Zhang, X. Huang, W. Guo, D. Dang, R. Zou, D. Xia, Q. Xu and M. Liu, *Nano Lett.*, **17**, 2788 (2017); https://doi.org/10.1021/acs.nanolett.6b05004